

Invoking Ferroptosis and Photon-Controlled Pyroptosis via an Integrated Therapeutic System for Triple-Pathway Tumor Therapy

Xue Lou, ^{†a} Wenkai Liu, ^{†c} Mingwang Yang, ^a Hua Zhang, ^{*b} Jiangli Fan, ^{*a} Xiaojun Peng ^a

a State Key Laboratory of Fine Chemicals, Frontiers Science Center for Smart Materials Oriented Chemical Engineering, Dalian University of Technology, Dalian 116024, P. R., China

b School of Chemistry and Chemical Engineering, Henan International Joint Laboratory of Smart Molecules and Identification and Diagnostic Functions, Henan Normal University, Henan 453007, P. R., China

c College of Chemical Engineering and Environment, Weifang University of Science and Technology, Weifang 262700, P. R., China

^{††} X. Lou and W.K. Liu contributed equally to this work.

E-mail:

zh1106@htu.edu.cn

fanjl@dlut.edu.cn

Content

EXPERIMENTAL SECTIONS.....	5
Material characterization	5
The synthesis of Q2S.....	5
The synthesis of QSH	5
Cell lines.....	6
The generation of ROS in living cells.....	6
Cellular apoptosis detection.....	7
Organelle Colocalization Imaging Experiments	7
Mitochondrial Distribution.....	7
Intracellular LPO Assay	7
Intracellular GSH content	8
LDH release.....	8
Western blot analysis.....	8
Immunofluorescence Staining (CRT and HMGB1)	9
Secretion of ATP	9
4T1 tumor-bearing mice model establishment	9
Statistical Analysis	10
Figure S1. The synthesis route of QSH.....	11
Figure S2. The ¹H NMR of QSH.	11
Figure S3. The ¹³C NMR of QSH.	12
Figure S4. The HRMS of QSH.	12
Figure S5. a) Absorption spectra (inset) of QSH (10 μM) and QSH+GSH (2 mM) in aqueous solutions. c)	

fluorescence spectra (inset) of QSH (10 μ M) and QSH+GSH (2 mM) in aqueous solutions.....	12
Figure S6. a) Fluorescence changes of QSH over a 180-minute period; b) Solvent color of QSH before (blue) and after (green) reaction with GSH (2 mM).	13
Figure S7. DPBF photodegradation curves with QSH (1.5 μ M); QSH (1.5 μ M) + GSH (2 mM) under 690 nm light irradiation (0.05 W cm ⁻²) from 0 to 300 s; Time-dependent UV/vis spectra of DPBF at 410 nm in the absence or presence of GSH.....	13
Figure S8. The HPLC-HRMS analysis of QSH after reaction with GSH.	14
Figure S9. Fluorescence images of 4T1 cells incubated with QSH for different times.	14
Figure S10. Fluorescence images of MCF-7 cells incubated with QSH for different times.....	15
Figure S11. MTT of tumor cells treated with QSH for 24 h.....	15
Figure S12. a) Cell viability of A549 cells incubated with QSH with or without light irradiation (690 nm laser, 0.05 W cm ⁻² , 5 min) at various concentrations (n=3). b) Cell viability of HeLa cells incubated with QSH with or without light irradiation (690 nm laser, 0.05 W cm ⁻² , 5 min) at various concentrations (n=3). c) Cell viability of MCF-7 cells incubated with QSH with or without light irradiation (690 nm laser, 0.05 W cm ⁻² , 5 min) at various concentrations (n=3).	15
Figure S13. MTT of COS-7 cells treated with QSH for 24 h.....	16
Figure S14. The intracellular glutathione (GSH) levels in different cell lines (n=3).	16
Figure S15. fluorescence images and flow cytometry analysis of ROS production in MCF-7 cells.....	16
Figure S16. Visualization of QSH colocalization with mitochondria (Red: QSH; Green: Mito).....	17
Figure S17. CLSM images of mitochondrial distribution of 4T1 cells after treatment with various treatments.	17
Figure S18. CLSM images of mitochondrial distribution of MCF-7 cells after treatment with various treatments.	18
Figure S19. CLSM images of MCF-7 cells after various treatments stained with JC-1 for mitochondrial membrane potential.....	18
Figure S20. Intracellular GSH levels and MDA content in MCF-7 cells following various treatments.	19
Figure S21. Cellular LPO accumulations of 4T1 cells after co-incubation with various treatments.	19

Figure S22. Cellular LPO accumulations of MCF-7 cells after co-incubation with various treatments.	20
Figure S23. DIO staining for cell membrane integrity of 4T1 cells after various treatments.....	20
Figure S24. DIO staining for cell membrane integrity of MCF-7 cells after various treatments.	21
Figure S25. Uncropped western blot source data for Figure 3 and 4.	21
Figure S26. a) The Phototoxicity of QSH (690 nm, 0.05 W cm ⁻² , 5 min) on 4T1 cells with or without uridine (20 μM) pretreatment (n=3). b) The Phototoxicity of QSH (690 nm, 0.05 W cm ⁻² , 5 min) on 4T1 cells with or without Fer-1 (1 μM) pretreatment (n=3). c) Intracellular lipid peroxidation levels in 4T1 cells following co-treatment with Fer-1 (1 μM) and QSH+L (690 nm laser, 0.05 W cm ⁻² , 5 min) (n=3). **p<0.01.....	22
Figure S27. Confocal microscopic images indicating CRT exposure of 4T1 cells after various treatments.....	22
Figure S28. Confocal microscopic images indicating HMGB1 exposure of 4T1 cells after various treatments.	23
Figure S29. Confocal microscopic images indicating CRT exposure of MCF-7 cells after various treatments.....	23
Figure S30. Confocal microscopic images indicating HMGB1 exposure of MCF-7 cells after various treatments..	24
Figure S31. Secretion of ATP in the cell culture supernatant of MCF-7 cells after different treatments.	24
Figure S32. a) Phototoxicity of QSH (690 nm laser, 0.05 W cm ⁻² , 5 min) in 4T1 cells with Fer-1 (1 μM), Ac (5 μM) and in combination (n=3). b) Intracellular peroxide levels upon co-incubation with Fer-1 alone, Ac alone, or their combination (n=3). c) The level of LDH release in cells co-incubated with Fer-1 alone, Ac alone, or their combination (n=3). *p<0.05, **p<0.01, ***p<0.001.....	25
Figure S33. a) Bubble plot of enriched Gene Ontology (GO) terms in Biological Process (BP) and Molecular Function (MF) categories. b) Bubble plot of additional enriched Biological Process (BP) terms related to immune regulation and cellular stress responses.	26
Figure S34. After 14 days of treatment, photographs of tumors in different groups.	26
Figure S35. Uncropped western blot source data for Figure 6.	26
Figure S36. H&E images of heart, liver, spleen, lung and kidney from 4T1 tumor-bearing mice upon different treatments.....	27
Figure S37. blood biochemical index of 4T1-bearing tumor mice treated with various treatments.	27

Experimental Sections

Material characterization

¹H nuclear magnetic resonance (¹H NMR) and ¹³C NMR spectra of all compounds were detected by Bruker AvanceII500 MHz spectrometer. The mass spectrometric (MS) data were obtained with electrospray ionization (ESI)-high resolution mass spectrometry (HRMS) instruments. Absorption spectra were performed with a Lambda 60 UV-visible (UV-Vis) spectrophotometer (PerkinElmer, USA). And fluorescence spectra were tested in a VAEIAN CARY Eclipse fluorescence spectrophotometer (Serial No. FL0812-M018). The cell imaging experiments were performed on confocal laser scanning microscope (CLSM, Olympus FV3000, Japan). High performance liquid chromatography (HPLC) analysis was taken by Agilent A1100. Cytotoxicity assays were analyzed by Thermo Varioskan™ LUX multifunctional microplate reader (USA). Flow cytometry was analyzed by Attune NxT Acoustic Focusing Cytometer.

The synthesis of Q2S

Isatin (340 mg, 2.31 mmol) and 1-([1,1'-biphenyl]-4-yl) ethan-1-one (400 mg, 2.04 mmol) were dissolved in 6 mL of EtOH containing 2 mL of H₂O. Subsequently, KOH (460 mg, 8.22 mmol) was added and the resulting solution was refluxed for 48 h. After completion of the reaction, the mixture was concentrated in vacuo and redissolved in a mixture of 1 M NaOH/EtOAc. The aqueous layer was then washed with EtOAc (3×) and acidified by addition of HCl (pH=1) until precipitant was observed. The obtained precipitant was washed with diethyl ether to yield the final product Q (148 mg, 0.46 mmol, 20% yield). Q (652 mg, 2 mmol), SS (489 μL, 4 mmol), DCC (495 mg, 2.4 mmol), and DMAP (73 mg, 0.6 mmol) were dissolved in 20 mL THF and stirred overnight. The solution is then concentrated under vacuum. The residue was purified with flash column chromatography (silica gel, PE:EtOAc=4:1) to afford Q2S as a white solid (507 mg, 55%).^[47]

The synthesis of QSH

Compound 1 (IHcy) (50 mg, 0.07 mmol) and triethylamine (7 mg, 0.07 mmol) were dissolved in anhydrous dichloromethane (DCM). The mixture was stirred under 0°C for 15 min under N₂ atmosphere and triphosgene

(20 mg, 0.07 mmol) was introduced for another 15 min reaction. Then Q2S (97 mg, 0.21 mmol) was added into the flask and the mixture was stirred at room temperature for 12 h. After removal of the solvent under reduced pressure, the residue was subjected to silica gel chromatography with CH₂Cl₂/CH₃OH (20/1, v/v) as the eluent. Finally, QSH as blue solid (46 mg, 60%) was afforded. ¹H NMR (400 MHz, Methanol-d₄) δ 8.61 (d, J = 8.0 Hz, 1H), 8.33 (s, 2H), 8.21 (d, J = 8.4 Hz, 2H), 8.04 (d, J = 8.2 Hz, 1H), 7.93 (d, J = 1.5 Hz, 1H), 7.82 (d, J = 8.3 Hz, 1H), 7.77-7.72 (m, 3H), 7.63-7.54 (m, 4H), 7.43-7.38 (m, 2H), 7.36 (d, J = 7.1 Hz, 1H), 7.20 (d, J = 8.4 Hz, 1H), 6.96 (s, 1H), 6.89 (s, 2H), 6.20 (d, J = 14.4 Hz, 1H), 4.71 (t, J = 7.1 Hz, 2H), 4.53 (t, J = 5.7 Hz, 2H), 4.10 (dd, J = 7.2, 2.4 Hz, 2H), 3.18 (t, J = 5.7 Hz, 2H), 2.72-2.66 (m, 2H), 2.59 (t, J = 6.0 Hz, 2H), 2.03 (d, J = 15.0 Hz, 2H), 1.96-1.91 (m, 2H), 1.62 (s, 6H), 1.36 (d, J = 4.9 Hz, 3H).^[48]

Cell lines

Mouse breast cancer cells (4T1 cells), human breast cancer cells (MCF-7 cells), mouse colorectal carcinoma cells (CT26 cells), human hepatocarcinoma Cells (HepG2 cells) and African green monkey kidney cells (COS-7 cells) were incubated at 37°C under a humidified atmosphere containing 5% CO₂, which were purchased from Institute of Basic Medical Sciences (IBMS) of the Chinese Academy of Medical Sciences. All cell lines except CT26 were cultured in Dulbecco's modified Eagle's medium (DMEM; C11995500BT, Gibco) supplemented with 10% (vol/vol) fetal bovine serum (FBS; 16000-044, Gibco) and 1% (vol/vol) penicillin/streptomycin solution (ST488-1/ST488-2, Beyotime). CT26 were cultured in Roswell Park Memorial Institute Medium (1640; C8016, Adamas). All cell lines were cultured at 37°C in a humidified atmosphere containing 5% CO₂ and were regularly tested for the absence of mycoplasma and bacterial contamination.

The generation of ROS in living cells

The reactive oxygen species (ROS) probe 2',7'-dichlorodihydrofluorescein diacetate (DCFH-DA, Ex: 488 nm, Em: 500-560 nm) was employed to detect ROS generation induced by QSH in living cells. 4T1 cells were seeded in glass-bottom culture dishes and incubated for 24 h at 37°C. Subsequently, the cells were treated with PBS, Q, Q2S, or QSH (2.5 μM) for 4 h, followed by incubation with 10 mM DCFH-DA for an additional 20 min. For the QSH+L group, cells were exposed to light irradiation (690 nm, 0.05 W cm⁻²) for 5 min after treatment. Intracellular ROS levels in all cell groups were then assessed using a confocal laser scanning microscope

(CLSM).

Cellular apoptosis detection

Cell death processes were visualized using the Calcein-AM/PI Apoptosis Detection Kit. 4T1 or MCF-7 cells were seeded in glass-bottom culture dishes and incubated in a humidified 5% CO₂ atmosphere at 37°C for 24 h. After treatment with QSH (2.5 μM) for 4 h, cells were irradiated with 690 nm light (0.05 W cm⁻², 5 min) and further incubated for 2 h. Untreated cells (blank control) and cells treated with QSH alone (2.5 μM) served as control groups. Subsequently, cells were stained with Calcein-AM and propidium iodide (PI) according to the manufacturer's instructions. The cell death process was then imaged under a confocal laser scanning microscope (CLSM) using a 60× objective lens.

Organelle Colocalization Imaging Experiments

For the organelle colocalization imaging experiments, 4T1 cells or MCF-7 cells (2×10⁵ cells/well) were seeded into a glass-bottom cell cultured for 24 h. Then, the cells were incubated with QSH (2.5 μM) for different time periods. After that, the cells were rinsed twice with PBS and stained by Mito-Tracker Green (λ_{ex}=488 nm; λ_{em}=500-560 nm). The intracellular fluorescence was imaged with the CLSM imaging system, and the corresponding Pearson's correlation coefficient (R) values were quantified via ImageJ software.

Mitochondrial Distribution

To investigate whether QSH can reduce the number of mitochondria, 4T1 cells or MCF-7 cells (3×10⁵ cells/well) were seeded in confocal dishes for 24 h. Then, the cells were incubated with different treatments, including PBS, Q, Q2S, and QSH (at a concentration of 2.5 μM) for 4 h and then QSH+L-treated cells were exposed to laser irradiation (690 nm, 0.05 W cm⁻²) for 5 min. After washing with PBS, cells were stained with Mito-Tracker Green and detected by fluorescence microscopy (λ_{ex}=488nm; λ_{em}=500-560nm).

Intracellular LPO Assay

4T1 cells and MCF-7 cells were seeded into confocal dishes at a density of 2×10⁴ cells/well and cultured for 24 h, and the medium was discarded. Then, the cells were incubated with PBS, Q, Q2S, and QSH (2.5 μM) for 4 h

and then QSH+L-treated cells were exposed to laser irradiation (690 nm, 0.05 W cm⁻²) for 5 min. Subsequently, the cells were incubated with C11-BODIPY581/591. Additionally, liperfluo was used to detect intracellular LPO levels by the CLSM imaging system, and the Malondialdehyde (MDA) amount was monitor educing an MDA assay kit.

Intracellular GSH content

4T1 cells or MCF-7 cells were seeded in 6-well plates at 5.0×10⁵ cells per well and cultured with PBS, Q, Q2S, and QSH (2.5 μM) for 4 h and then QSH+L-treated cells were exposed to laser irradiation (690 nm, 0.05 W cm⁻²) for 5 min. The culture medium was replaced by fresh DMEM to remove the residual medicine. The GSH amount was evaluated using GSH assay kit.

LDH release

Extracellular secretion of LDH was tested using an LDH assay kit. Briefly, 4T1 cells or MCF-7 cells were seeded into a 6-well at a density of 1×10⁵ cells each well and incubated overnight. And then cells were incubated with PBS, Q, Q2S, and QSH (2.5 μM) for 4 h and then QSH+L-treated cells were exposed to laser irradiation (690 nm, 0.05 W cm⁻²) for 5 min. After 1 h, the supernatants were collected and then conducted with centrifugation using 12,000 rpm for 10 min at 4 °C. The level of released LDH was quantitatively determined by LDH bioluminescent assay kit according to manufacturer's instruction.

Western blot analysis

4T1 cells or MCF-7 cells were seeded into 6-well plates at a density of 5 × 10⁵ cells/well and cultured for 24 h, and the medium was discarded. Then, the cells were incubated with PBS, Q, Q2S, QSH (2.5 μM) for 4 h and then QSH+L-treated cells were exposed to laser irradiation (690 nm, 0.05 W cm⁻²) for 5 min. The cells were resuspended in lysis buffer. Subsequently, the extracted protein (15 μL) was analyzed by electrophoresis running on 12% denaturing polyacrylamide gels. The proteins were then transferred to PVDF membranes, followed by blocking with 5% skim milk powder for 1h. The membranes were then incubated with primary antibodies (1: 20,000 in 2% skim milk) (mouse monoclonal antibody, Abcam) overnight at 4°C, followed by washing with TBST buffer thrice. The membranes were further incubated with horseradish peroxidase-conjugated

secondary antibody (1:20,000, goat anti-mouse IgG, proteintech) for 2h at room temperature, and then were washed with TBST buffer thrice. The protein bands were visualized using ECL reagent under ChemiDoc XR+ system (Bio-rad).

Immunofluorescence Staining (CRT and HMGB1)

4T1 cells or MCF-7 cells were spread evenly on the confocal chamber (5×10^4 cells per well). After cell attachment, the cells were incubated with PBS, Q, Q2S, QSH (2.5 μ M) for 4 h and then QSH+L-treated cells were exposed to laser irradiation (690 nm, 0.05 W cm^{-2}) for 5 min. Subsequently, cells underwent washing fixation-washing-permeabilization-washing-blocking for staining. Next, cells were incubated with primary antibody (1:400 dilution) at 4°C overnight. The next day, the primary antibody was recovered and the immunofluorescent secondary antibody (1:400 dilution) was incubated at room temperature for 60 min, and the nuclei were stained with DAPI for 15 min. Finally, CLSM was used for observation.

Secretion of ATP

4T1 cells or MCF-7 cells were seeded into 6-well plates at a density of 5×10^5 cells/well and cultured for 24 h, and the medium was discarded. Then, the cells were incubated with PBS, Q, Q2S, QSH (2.5 μ M) for 4 h and then QSH+L-treated cells were exposed to laser irradiation (690 nm, 0.05 W cm^{-2}) for 5 min. Subsequently, the level of released ATP was quantitatively determined by ATP assay kit according to manufacturer's instruction.

4T1 tumor-bearing mice model establishment

To establish the 4T1 tumor-bearing mice model, the cells (about 5×10^5) were inoculated subcutaneously into the right thigh of the mice. Once the tumor volume reached $\sim 80 \text{ mm}^3$, the mice were used for subsequent experiments. The tumor volume was estimated by the formula: $V = L \times D^2/2$, in which L and D was the longest and the shortest diameter of the tumor, respectively. The tumor growth inhibition rate (TGIR) was calculated according to the following equation: $\text{TGIR} (\%) = (\text{WC} - \text{WT})/\text{WC} \times 100\%$, where WC was the tumor weight of the PBS group and WT represented the tumor weight of mice after the treatments. Survival was assessed using Kaplan Meier analysis (using OriginPro 2024 software).

Statistical Analysis

Fluorescence quantification of the confocal images was performed using ImageJ Fiji software, and colocalization analyses were defined using the Pearson correlation coefficient. All statistical analyses were performed using GraphPad Prism 9.0, and data were calculated and processed as mean \pm standard deviation (SD) in at least three independent experiments, the specific sample size (n) was illustrated in the figure legend. Statistical comparisons between two groups were made using two-tailed unpaired Student's t-tests, while multiple group comparisons were assessed using one-way ANOVA. Statistical significance was defined as $p < 0.05$; * $p < 0.05$, ** $p < 0.01$, and *** $p < 0.001$.

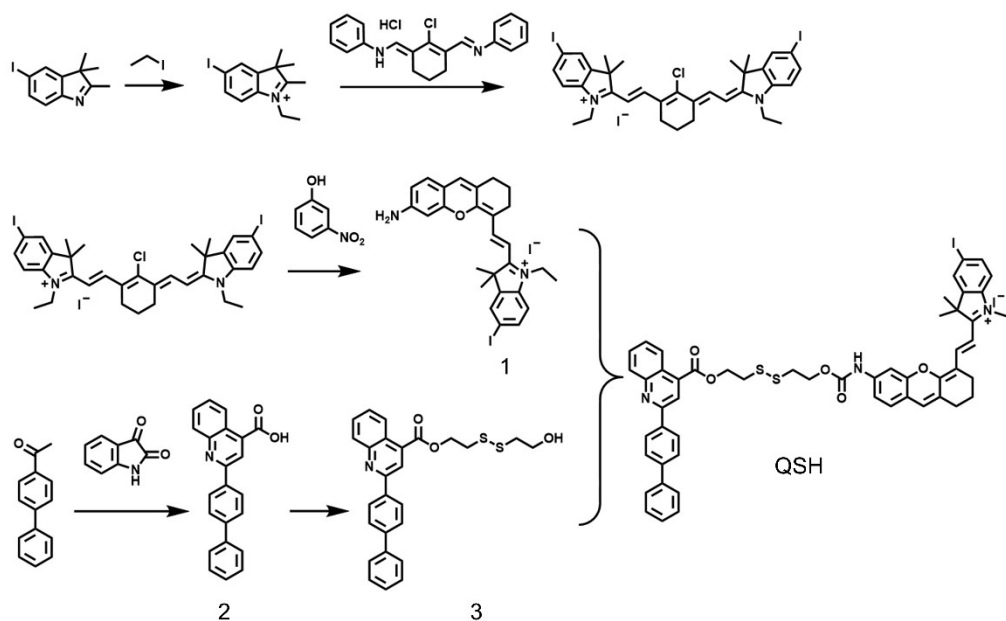


Figure S1. The synthesis route of QSH

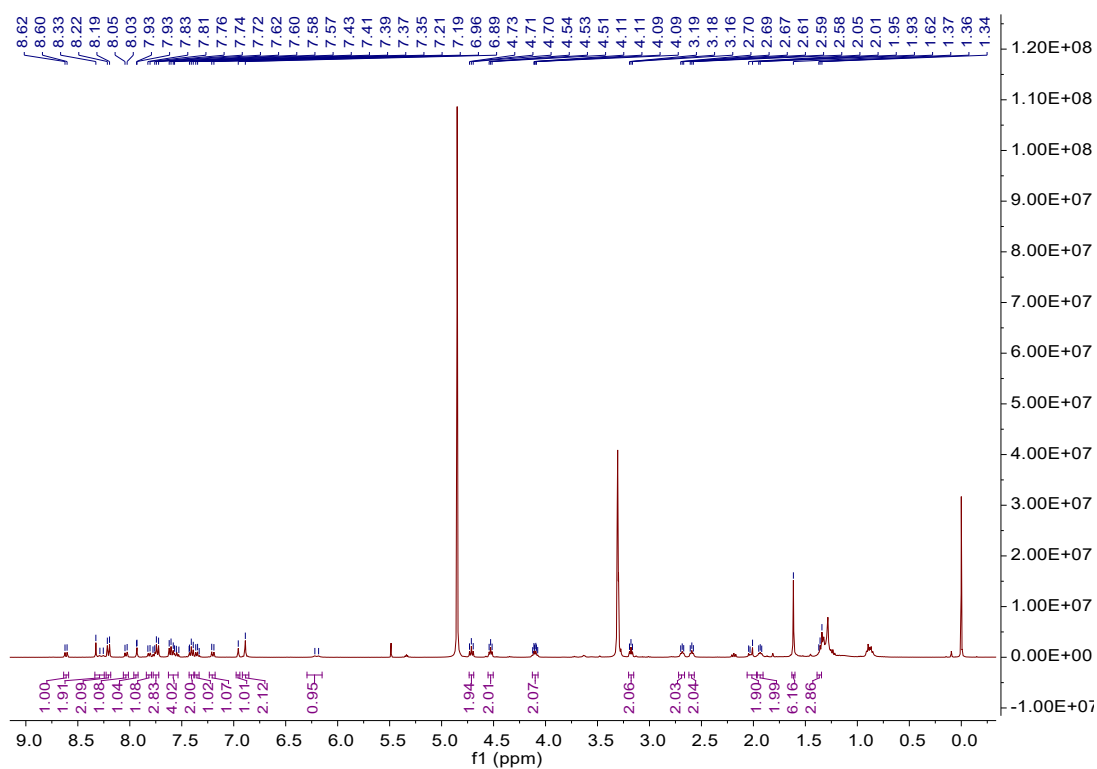


Figure S2. The ¹H NMR of QSH.

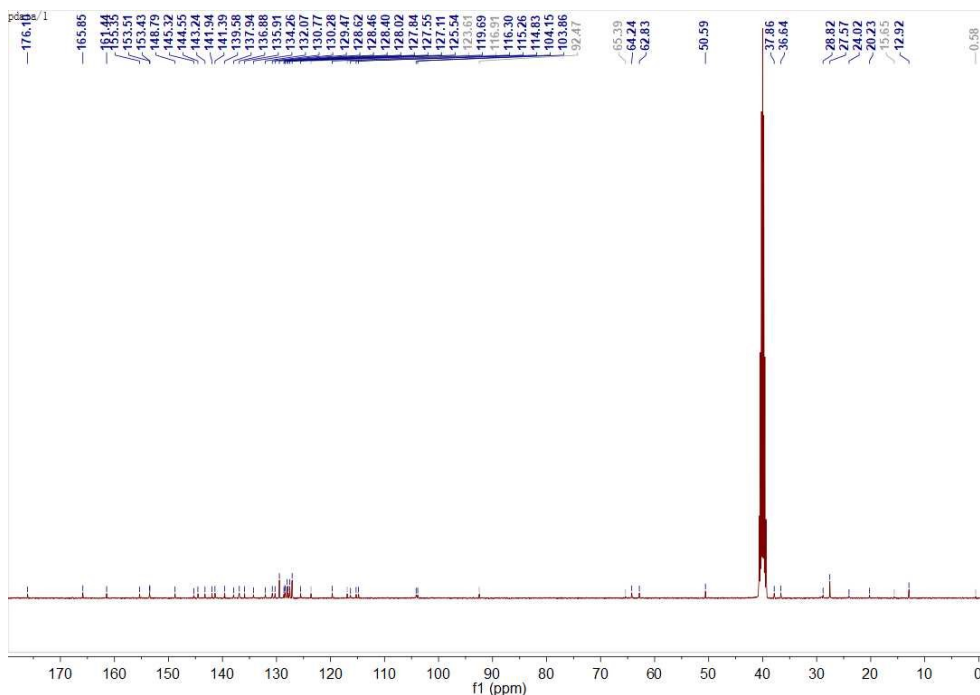


Figure S3. The ¹³C NMR of QSH.

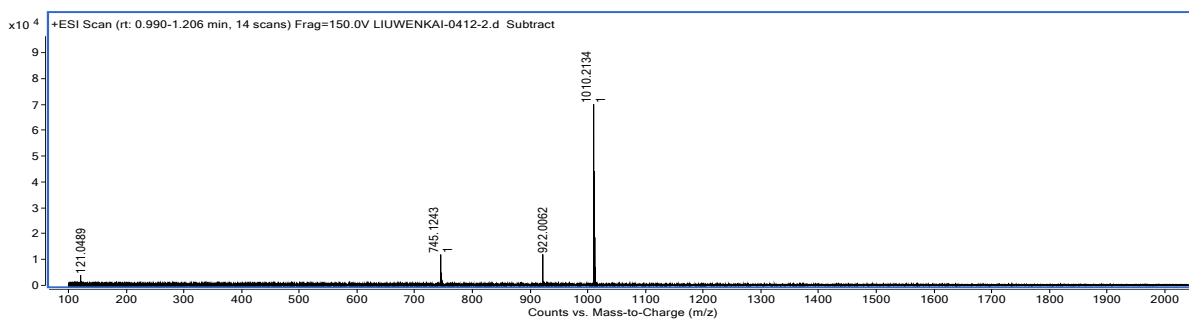


Figure S4. The HRMS of QSH.

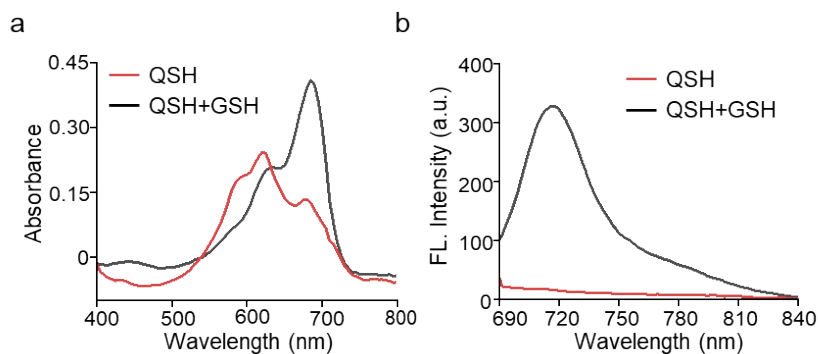


Figure S5. a) Absorption spectra (inset) of QSH (10 μ M) and QSH+GSH (2 mM) in aqueous solutions. c) fluorescence spectra (inset) of QSH (10 μ M) and QSH+GSH (2 mM) in aqueous solutions.

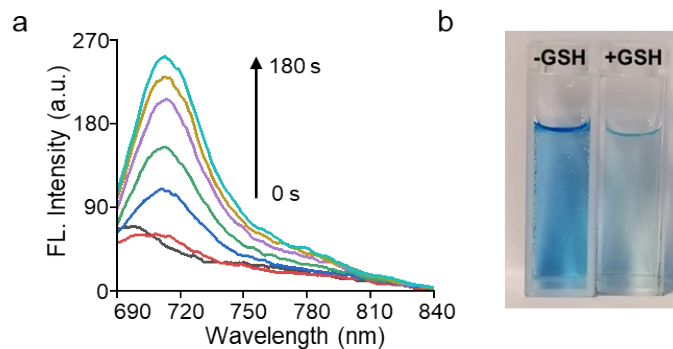


Figure S6. a) Fluorescence changes of QSH over a 180-minute period; b) Solvent color of QSH before (blue) and after (green) reaction with GSH (2 mM).

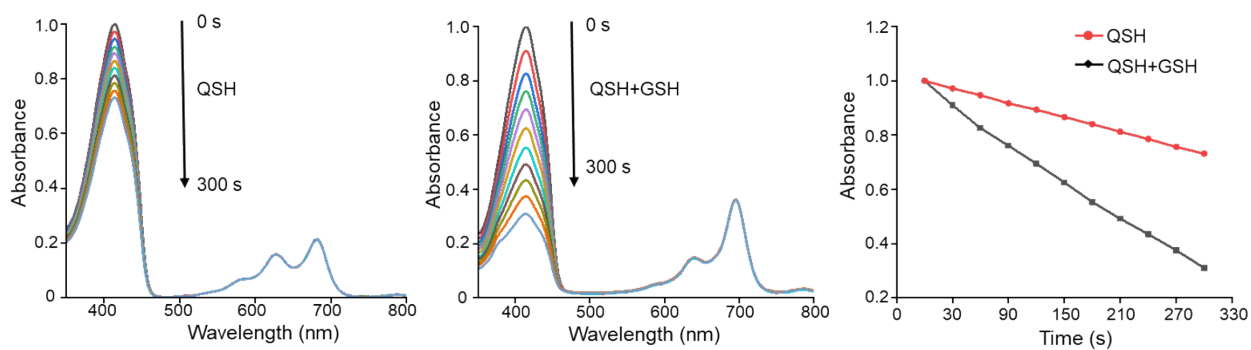
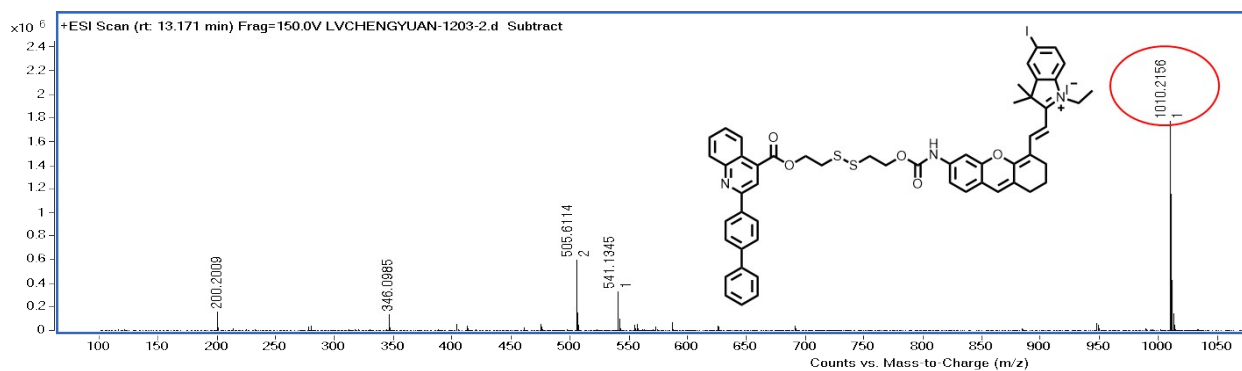


Figure S7. DPBF photodegradation curves with QSH (1.5 μM); QSH (1.5 μM) + GSH (2 mM) under 690 nm light irradiation (0.05 W cm^{-2}) from 0 to 300 s; Time-dependent UV/vis spectra of DPBF at 410 nm in the absence or presence of GSH.



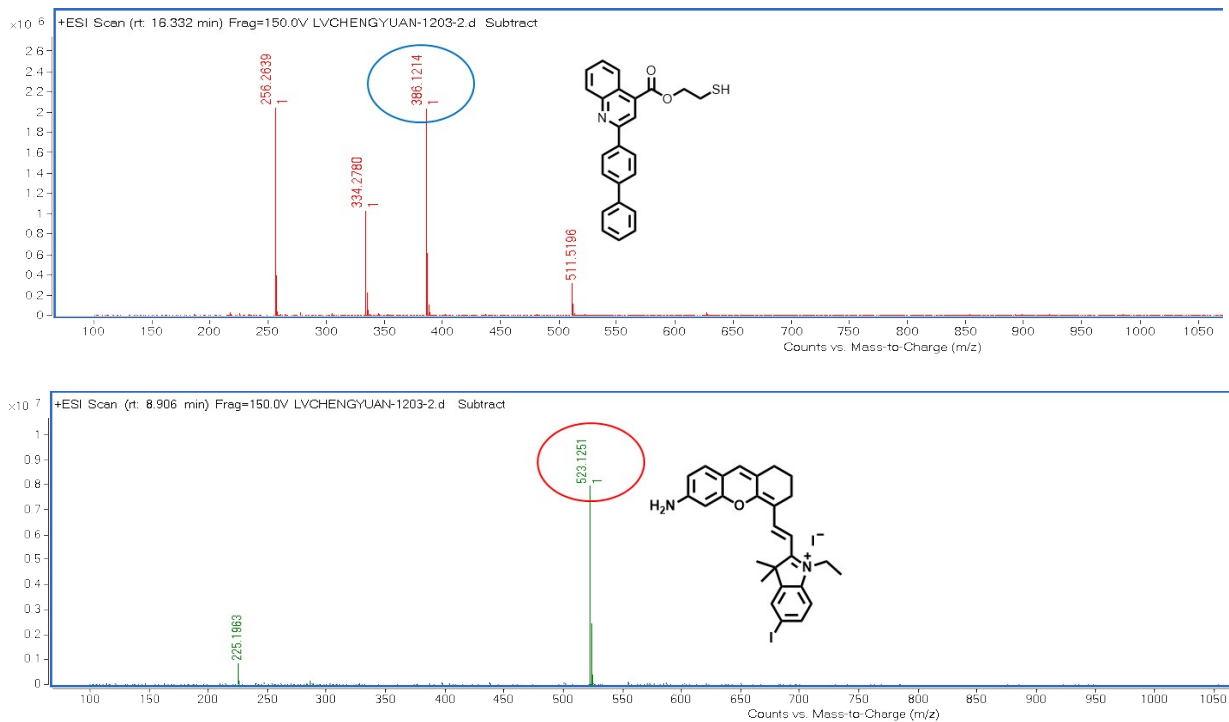


Figure S8. The HPLC-HRMS analysis of QSH after reaction with GSH.

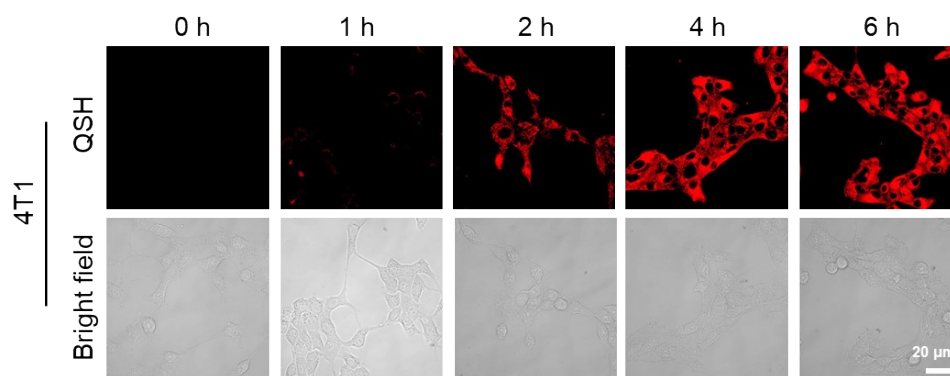


Figure S9. Fluorescence images of 4T1 cells incubated with QSH for different times.

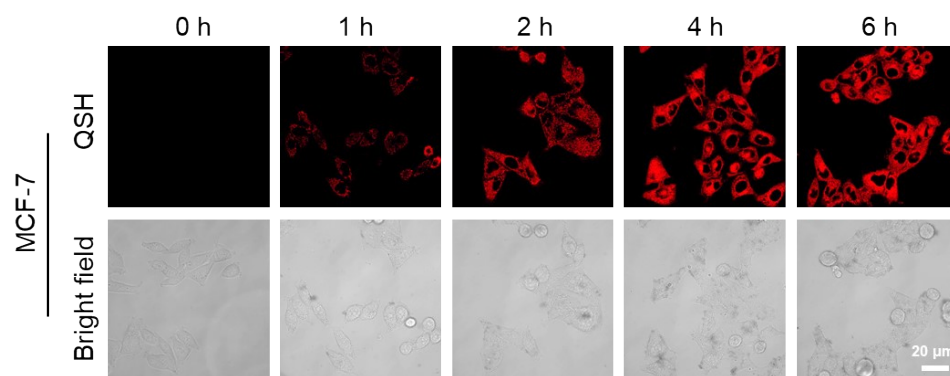


Figure S10. Fluorescence images of MCF-7 cells incubated with QSH for different times.

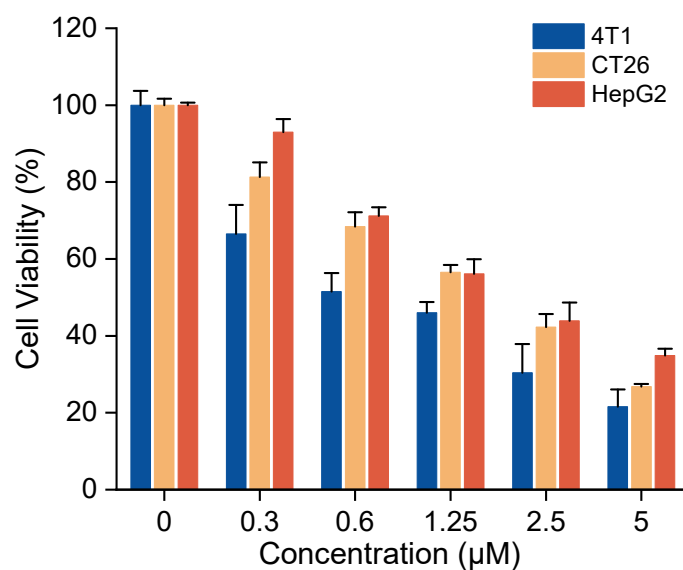


Figure S11. MTT of tumor cells treated with QSH for 24 h.

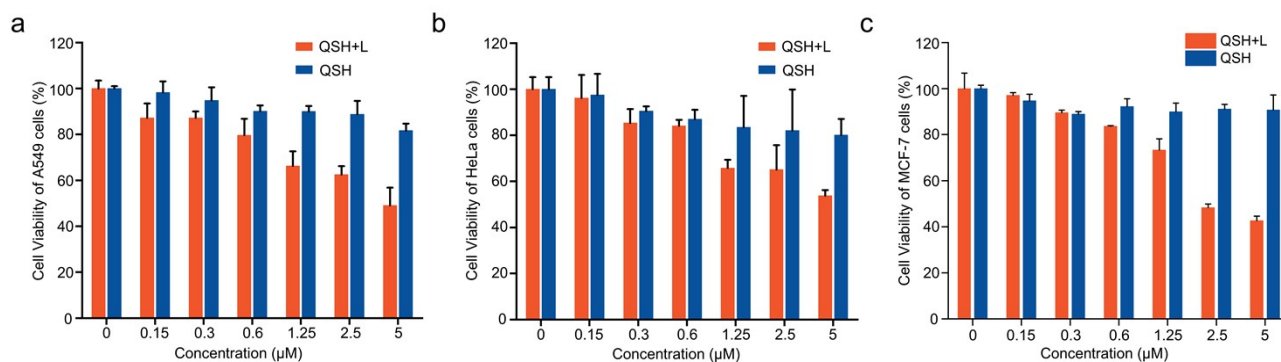


Figure S12. a) Cell viability of A549 cells incubated with QSH with or without light irradiation (690 nm laser, 0.05 W cm⁻², 5 min) at various concentrations (n=3). b) Cell viability of HeLa cells incubated with QSH with or without light irradiation (690 nm laser, 0.05 W cm⁻², 5 min) at various concentrations (n=3). c) Cell viability of MCF-7 cells incubated with QSH with or without light irradiation (690 nm laser, 0.05 W cm⁻², 5 min) at various concentrations (n=3).

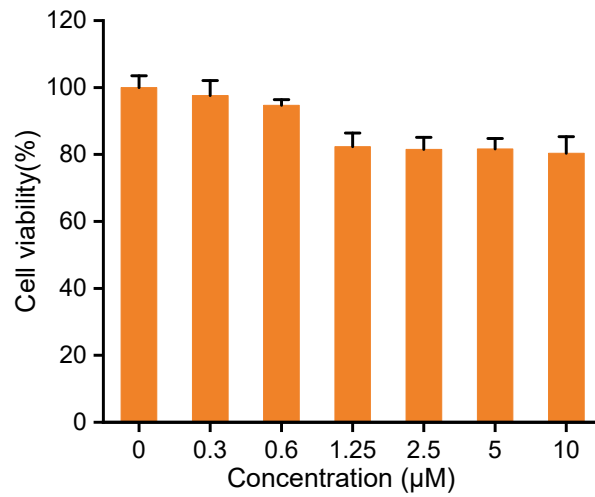


Figure S13. MTT of COS-7 cells treated with QSH for 24 h.

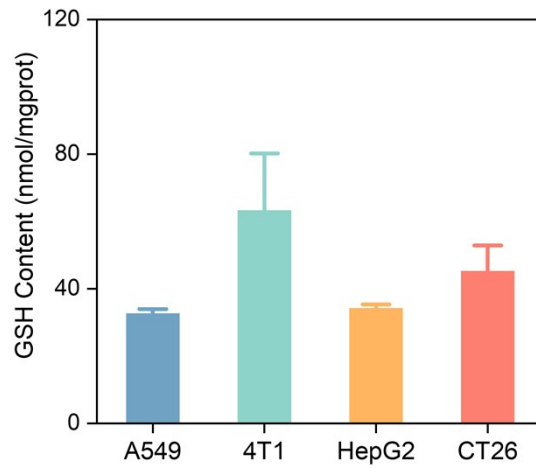


Figure S14. The intracellular glutathione (GSH) levels in different cell lines (n=3).

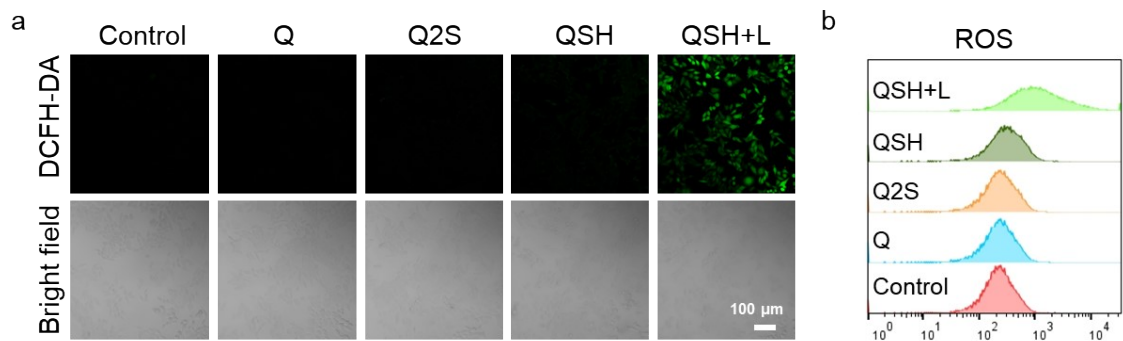


Figure S15. fluorescence images and flow cytometry analysis of ROS production in MCF-7 cells.

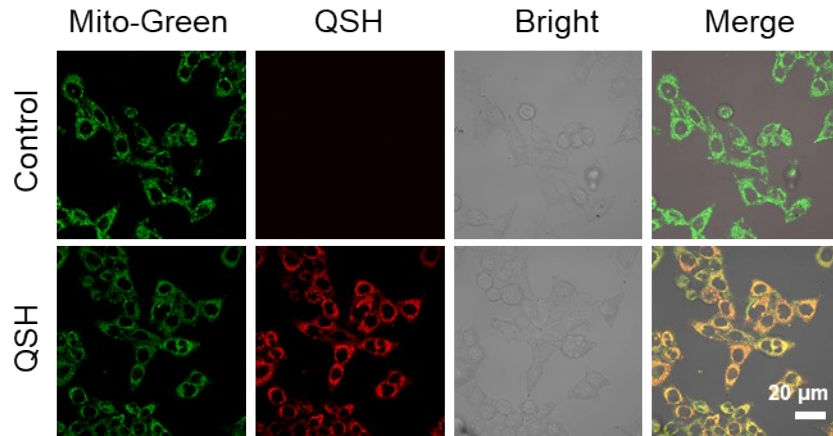


Figure S16. Visualization of QSH colocalization with mitochondria (Red: QSH; Green: Mito).

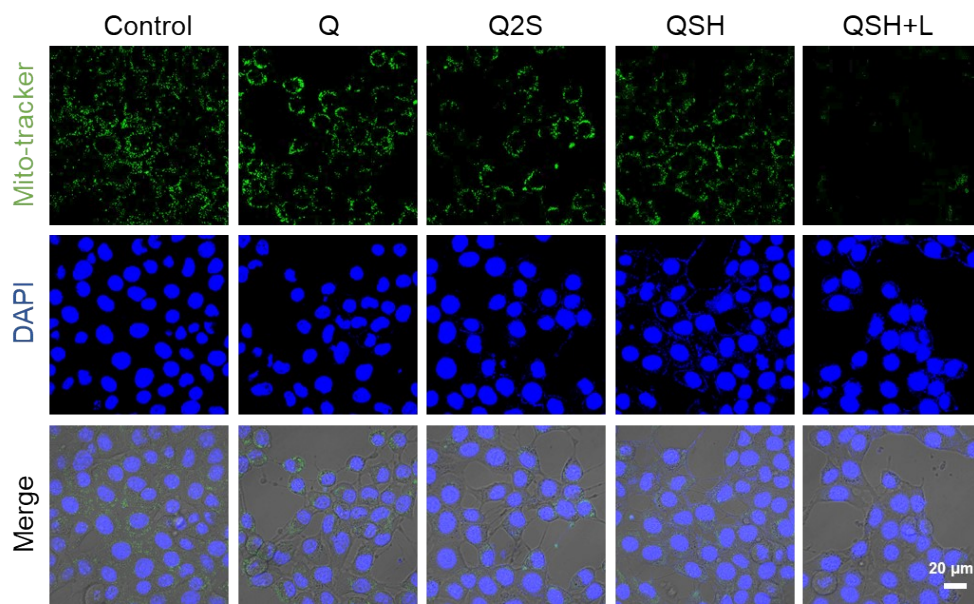


Figure S17. CLSM images of mitochondrial distribution of 4T1 cells after treatment with various treatments.

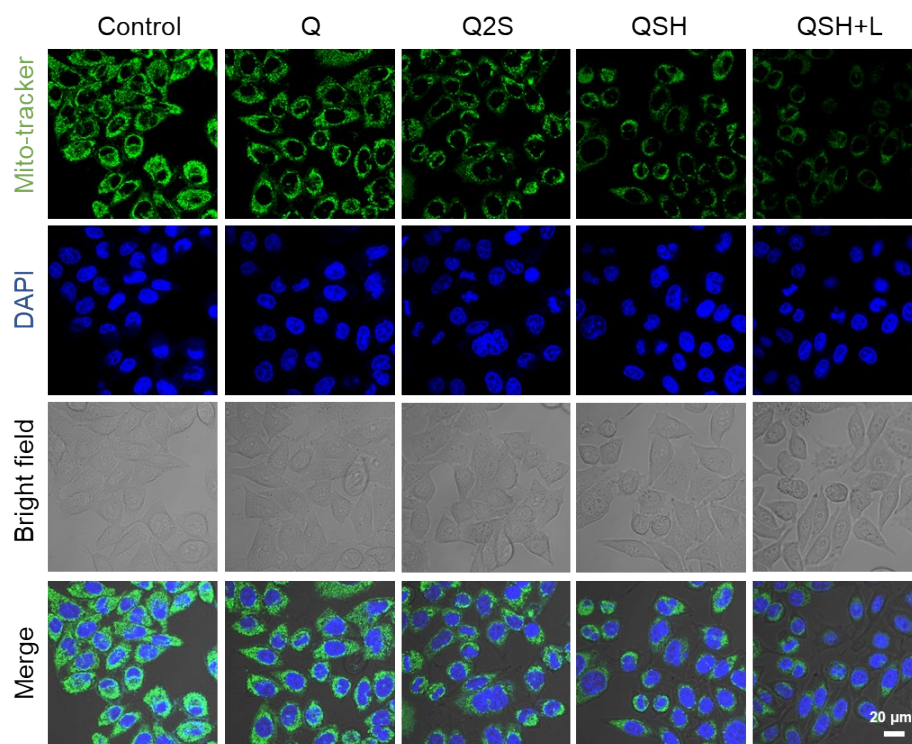


Figure S18. CLSM images of mitochondrial distribution of MCF-7 cells after treatment with various treatments.

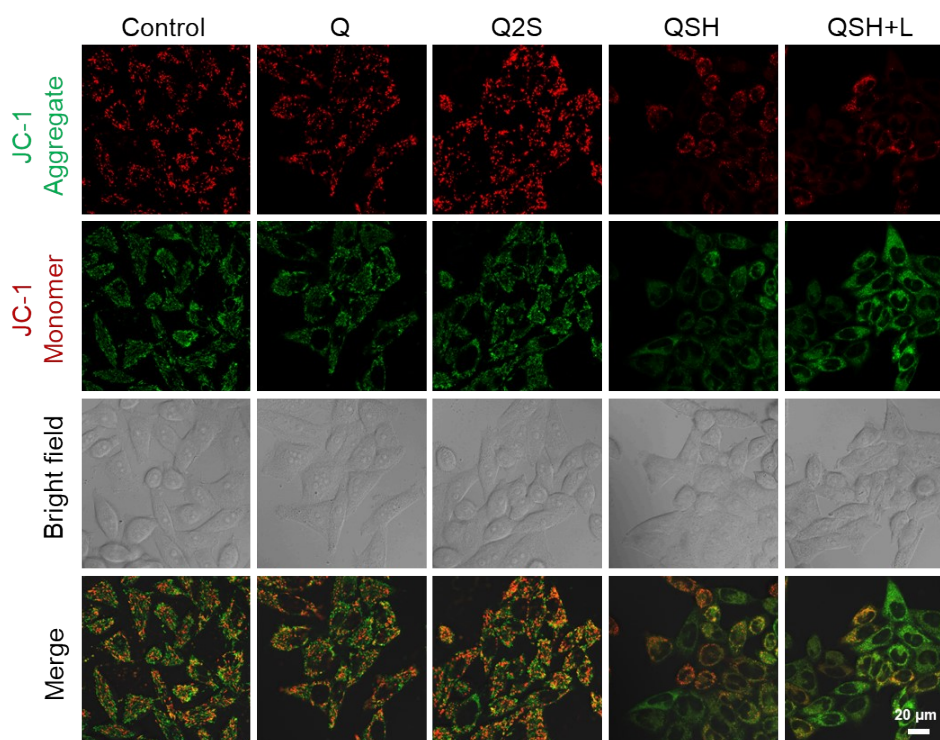


Figure S19. CLSM images of MCF-7 cells after various treatments stained with JC-1 for mitochondrial membrane potential.

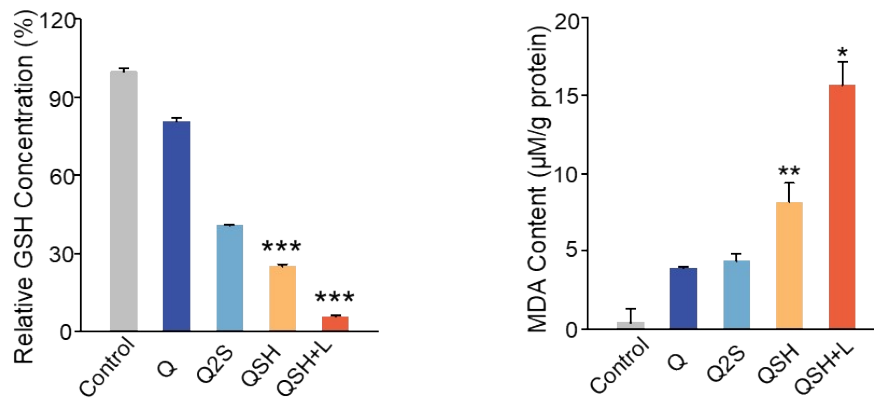


Figure S20. Intracellular GSH levels and MDA content in MCF-7 cells following various treatments. $*p<0.05$, $p<0.01$, $***p<0.001$.**

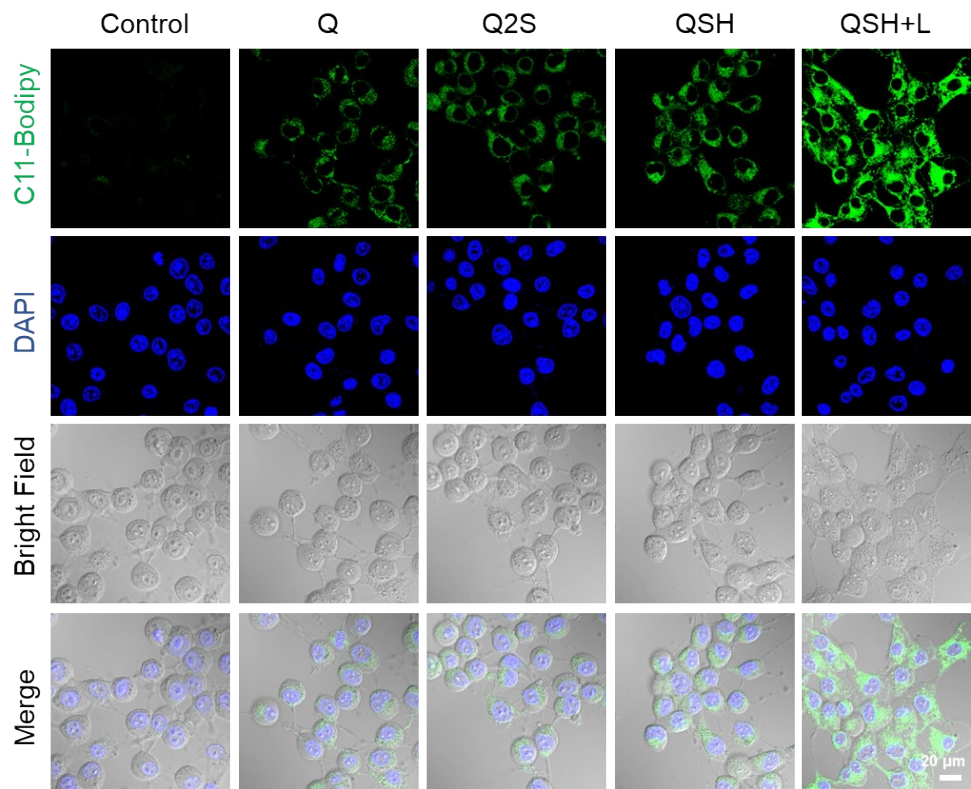


Figure S21. Cellular LPO accumulations of 4T1 cells after co-incubation with various treatments.

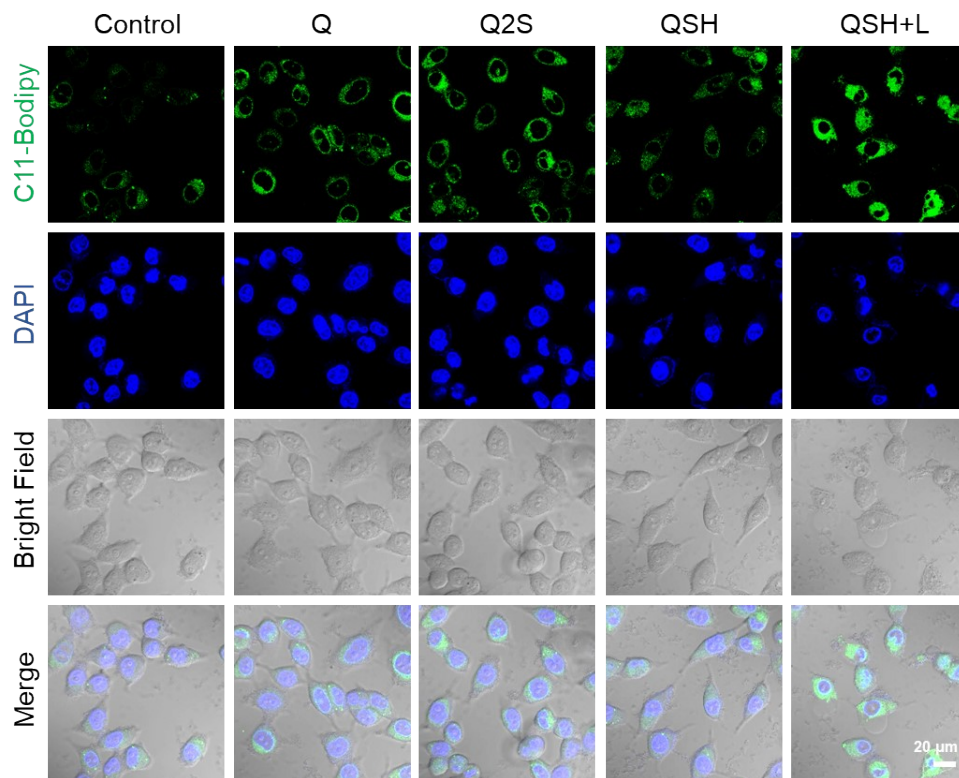


Figure S22. Cellular LPO accumulations of MCF-7 cells after co-incubation with various treatments.

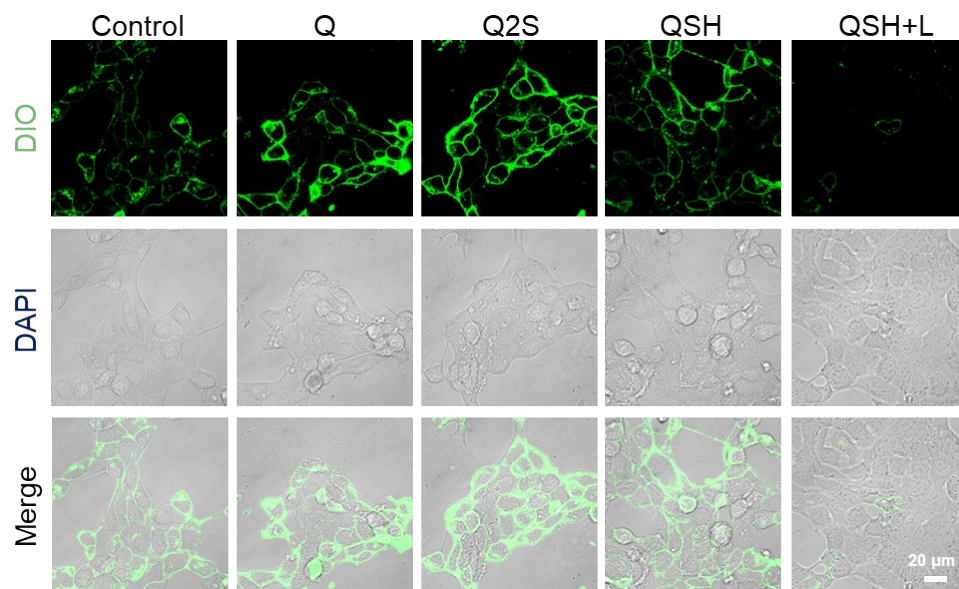


Figure S23. DIO staining for cell membrane integrity of 4T1 cells after various treatments.

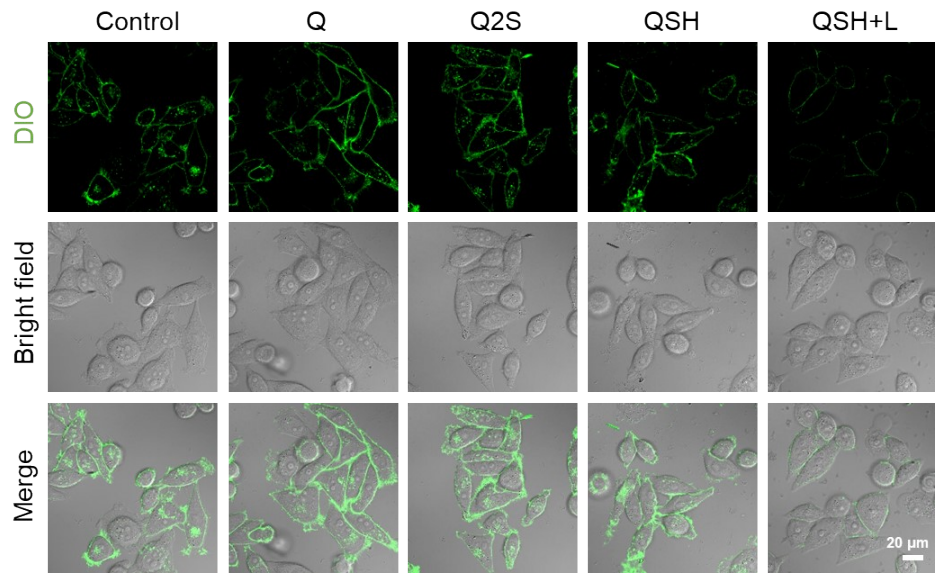


Figure S24. DIO staining for cell membrane integrity of MCF-7 cells after various treatments.

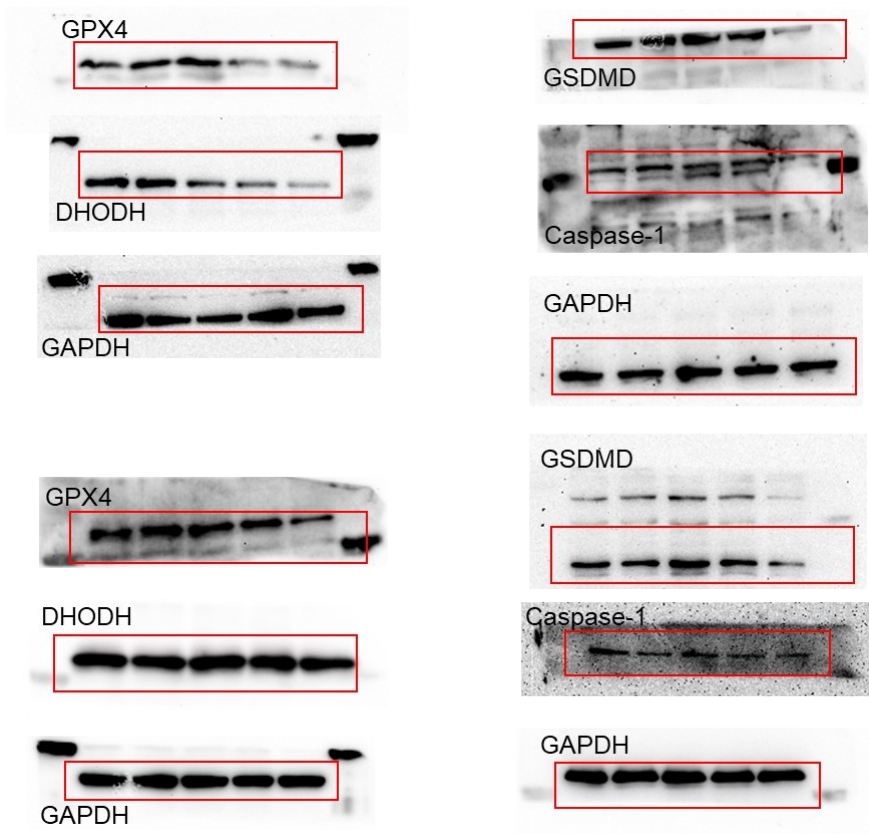


Figure S25. Uncropped western blot source data for Figure 3 and 4.

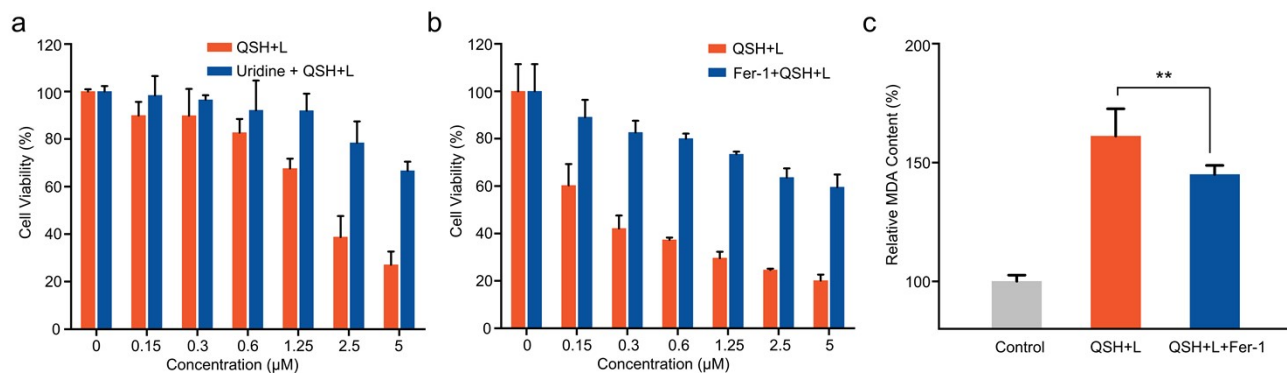


Figure S26. a) The Phototoxicity of QSH (690 nm, 0.05 W cm⁻², 5 min) on 4T1 cells with or without uridine (20 µM) pretreatment (n=3). b) The Phototoxicity of QSH (690 nm, 0.05 W cm⁻², 5 min) on 4T1 cells with or without Fer-1 (1 µM) pretreatment (n=3). c) Intracellular lipid peroxidation levels in 4T1 cells following co-treatment with Fer-1 (1 µM) and QSH+L (690 nm laser, 0.05 W cm⁻², 5 min) (n=3). *p*<0.01.**

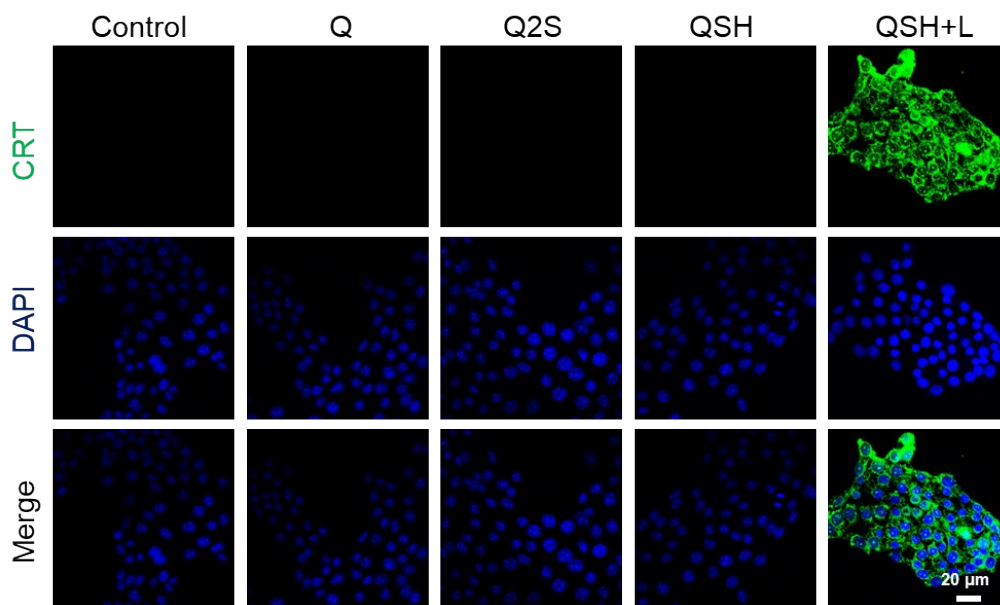


Figure S27. Confocal microscopic images indicating CRT exposure of 4T1 cells after various treatments.

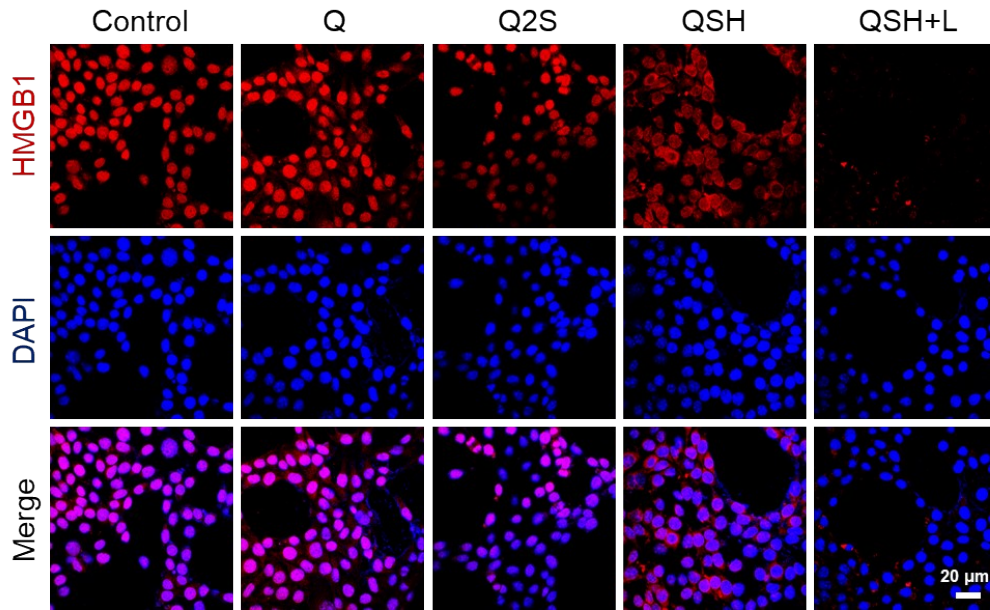


Figure S28. Confocal microscopic images indicating HMGB1 exposure of 4T1 cells after various treatments.

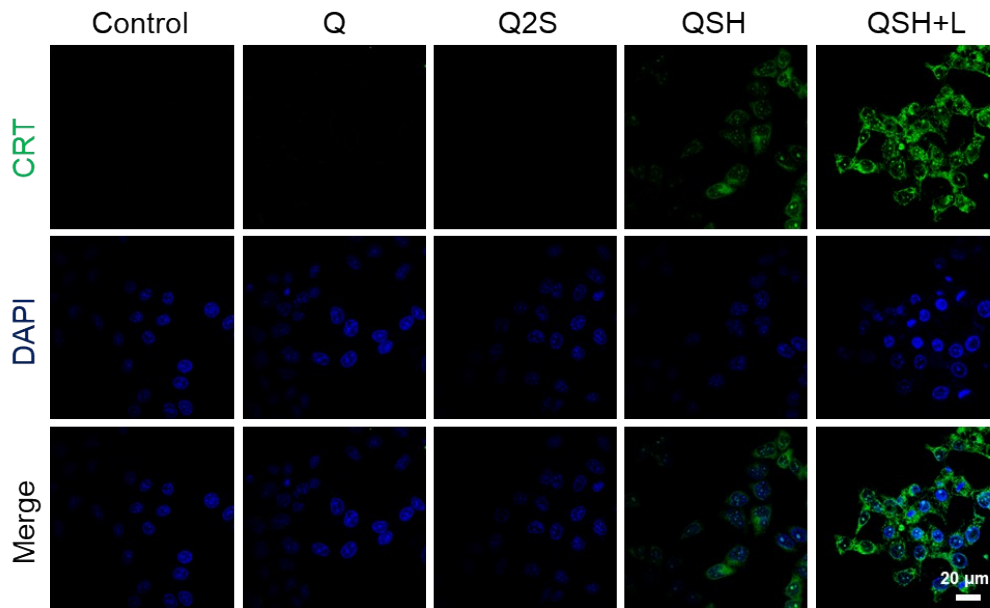


Figure S29. Confocal microscopic images indicating CRT exposure of MCF-7 cells after various treatments.

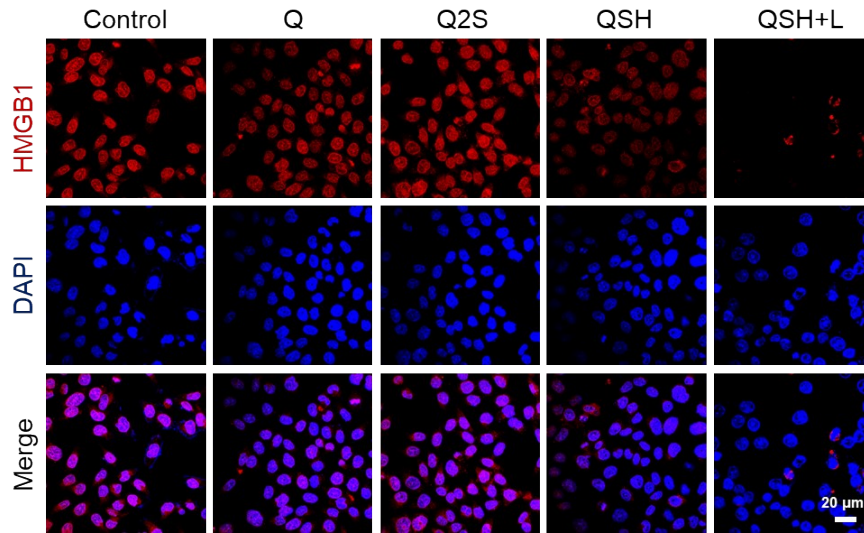


Figure S30. Confocal microscopic images indicating HMGB1 exposure of MCF-7 cells after various treatments.

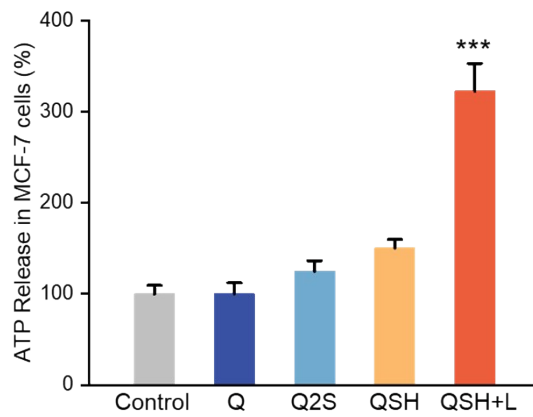


Figure S31. Secretion of ATP in the cell culture supernatant of MCF-7 cells after different treatments. *** $p < 0.001$.

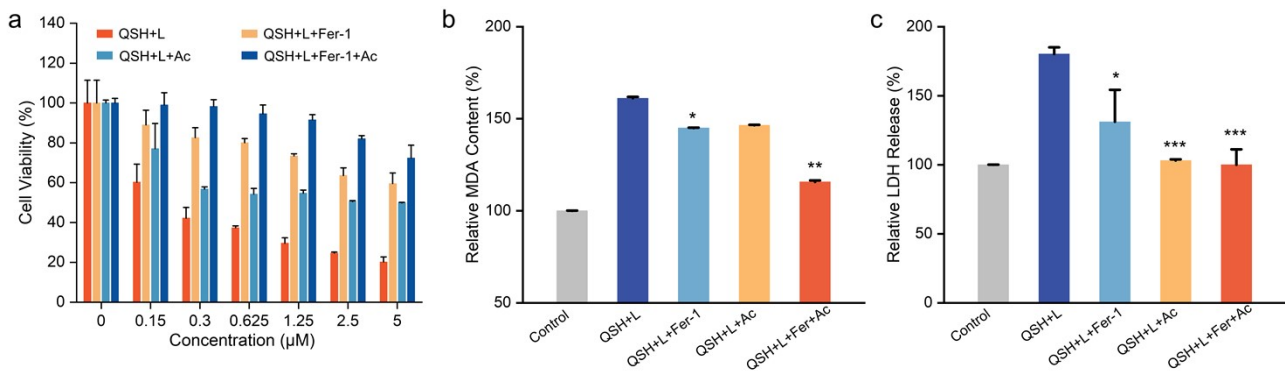


Figure S32. a) Phototoxicity of QSH (690 nm laser, 0.05 W cm⁻², 5 min) in 4T1 cells with Fer-1 (1 μM), Ac (5 μM) and in combination (n=3). b) Intracellular peroxide levels upon co-incubation with Fer-1 alone, Ac alone, or their combination (n=3). c) The level of LDH release in cells co-incubated with Fer-1 alone, Ac alone, or their combination (n=3). **p*<0.05, *p*<0.01, ****p*<0.001.**

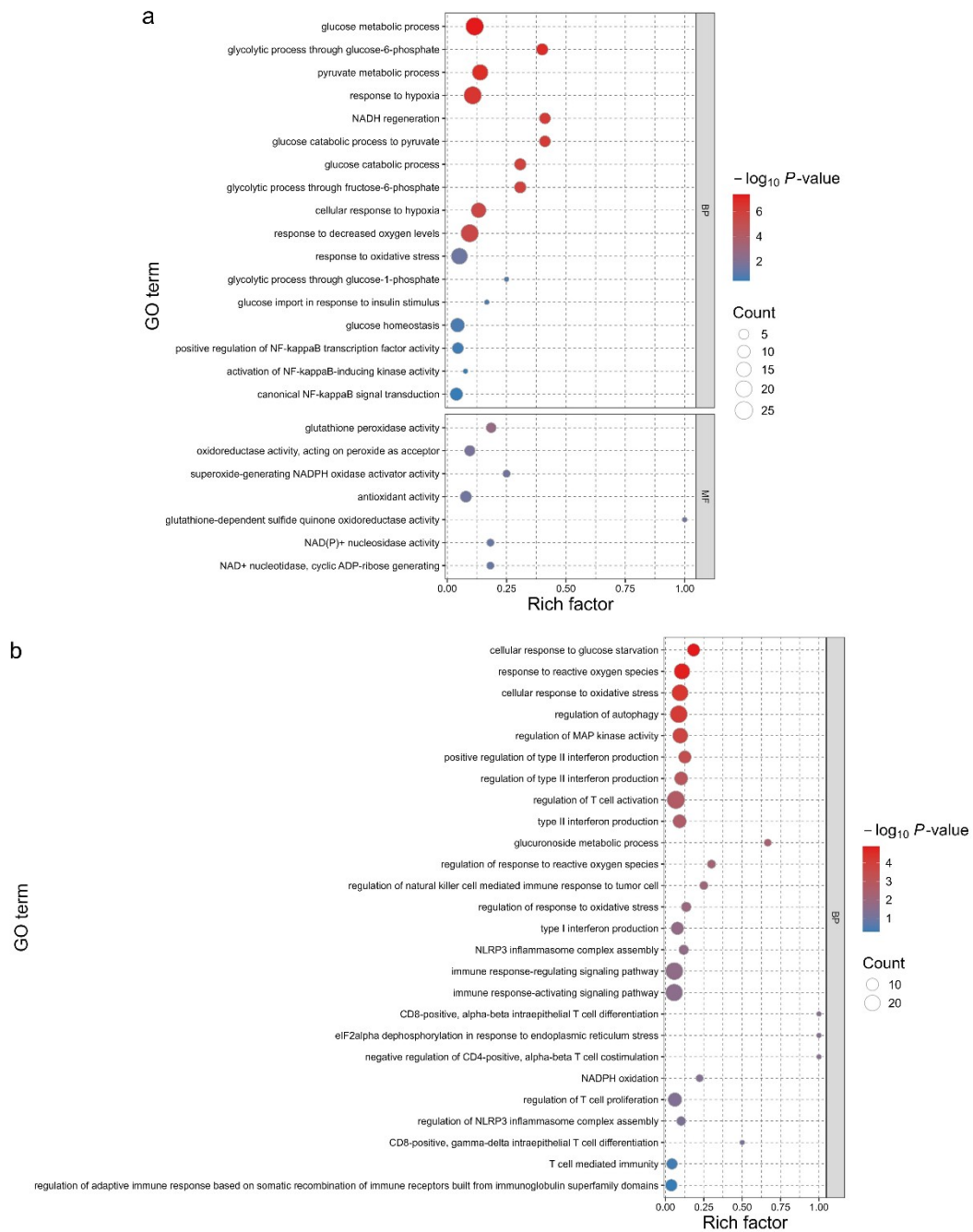


Figure S33. a) Bubble plot of enriched Gene Ontology (GO) terms in Biological Process (BP) and Molecular Function (MF) categories. b) Bubble plot of additional enriched Biological Process (BP) terms related to immune regulation and cellular stress responses.

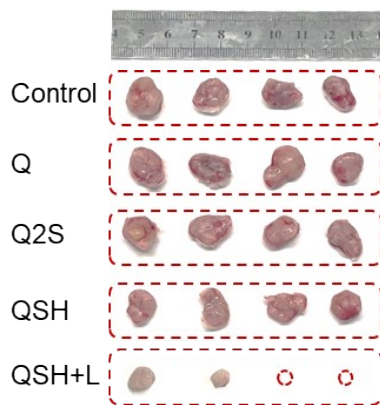


Figure S34. After 14 days of treatment, photographs of tumors in different groups.

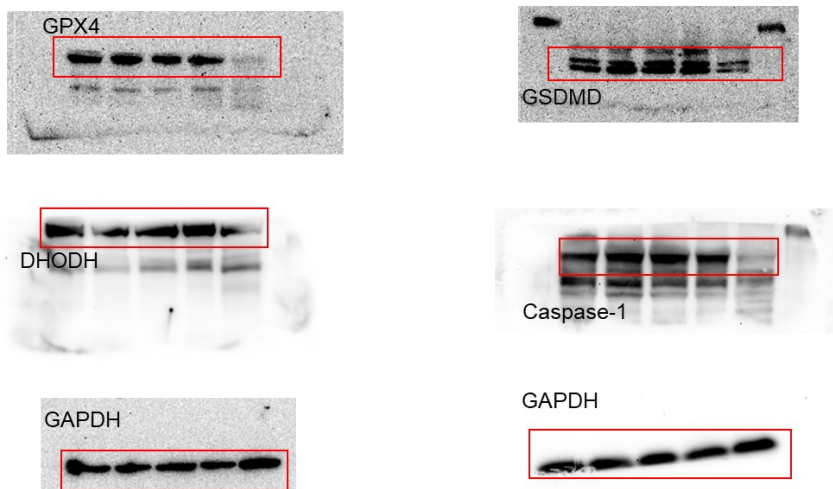


Figure S35. Uncropped western blot source data for Figure 6.

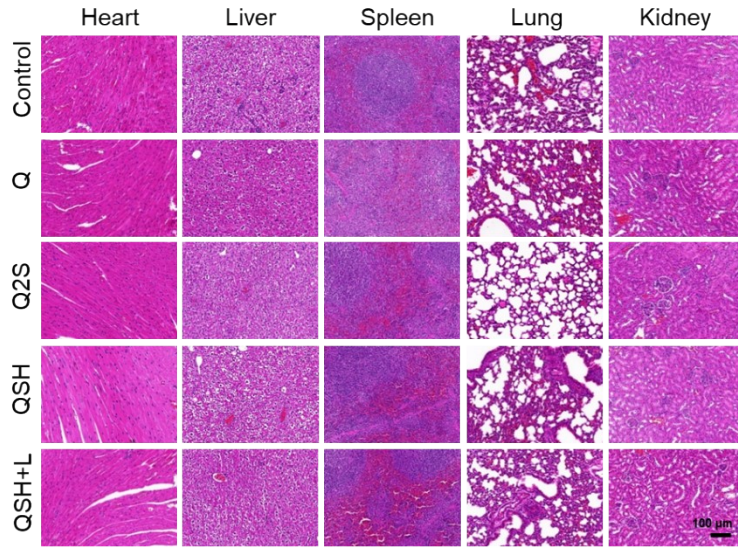


Figure S36. H&E images of heart, liver, spleen, lung and kidney from 4T1 tumor-bearing mice upon different treatments.

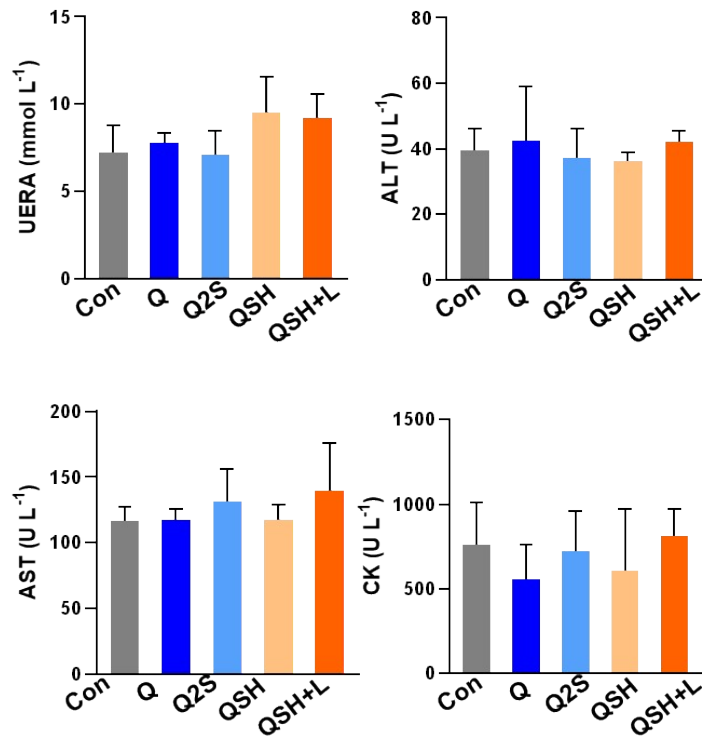


Figure S37. blood biochemical index of 4T1-bearing tumor mice treated with various treatments.